An Adaptive Backstepping Flux Observer for two Nonlinear Control Strategies Applied to WGS based on PMSG

Emna MAHERSI*, Adel KHEDER**‡

*Unit Research on Advanced Systems in Electrical Engineering, "SAGE".

University of Monastir, National Engineering School of Monastir,Tunisia

**Unit Research on Advanced Systems in Electrical Engineering, "SAGE".

University of Sousse, National Engineering School of Sousse, Tunisia

emna.mahersi@yahoo.fr, adel_kheder@yahoo.fr

‡ Corresponding Author; Adel KHEDER, Riadh 5 City Sousse 4023, Tunisia, Tel: +216 98 229 960

Abstract- A nonlinear backstepping flux observer (BFO) for two control strategies applied to directly driven wind synchronous generator is discussed. The proposed non linear control strategies are the backstepping control (BC) and the sliding mode control (SMC) applied to both converters: the stator side converter (SSC) and the grid side converter (GSC). The estimation of the stator flux via the BFO is provided by an adaptive mechanism of stator resistance using *Lyapunov* theory. The efficiency of the two non linear control strategies has been proved through computer simulations in terms of tracking ability, precision and robustness against resistance variations. Then, a comparative study between four possible combinations of control is illustrated and simulation results have shown high performances of the wind system controlled by BC strategy.

Keywords- Permanent Magnet Synchronous Generator, Wind turbine, Backstepping Control, Sliding Mode Control, Backstepping Flux Observer.

Nomenclature

T_{em}:	Electromagnetic torque (N.m),	n_p:	Pole pairs number,
T_m :	Turbine torque (N.m),	φ_r :	Rotor flux (Wb),
Ω_r :	Rotational speed (rad/s),	v_d, v_q:	Direct and quadrature stator voltages (V),
$\omega_r = n_p\Omega_r$	Electrical pulsation (rad/s),	i_d, i_q:	Direct and quadrature stator currents (A),
K_f :	Friction coefficient,	φ_d, φ_q:	Direct and quadrature stator fluxes (Wb),
J:	Moment of inertia,	R_s:	Stator resistance (Ω),
R_t:	Blade radius (m),	L_d, L_q:	Direct and quadrature stator inductances (H),
C_p:	Power coefficient,	v_{ld}, v_{lq}:	Direct and quadrature line voltages (V),
λ:	Tip speed ratio,	v_{gd}, v_{gq}:	Direct and quadrature grid voltages (V),
β:	Pitch angle (rad),	i_{ld}, i_{lq}:	Direct and quadrature line currents (A),
ρ:	Air density (Kg/m3),	R_f :	Filter resistance (Ω),
V :	Wind speed (m/s),	L_f :	Filter inductance (H).

1. Introduction

With the development of the control technology and the electronic devices, wind energy conversion systems based on the PMSG have been gaining popularity. The PMSG is directly connected to the wind turbine, then, the absence of the gearbox reduces the cost, the encumbrance and the maintenance of the system. The compact size, the high torque to inertia ratio and the ease of control make the PMSG required for wind generation systems [1, 2].

PMSG is nonlinear multivariable dynamic system, thus, various control strategies have been developed. The vector control strategy is the most widely applied to control the PMSG [3, 4]. With the nonlinearity presented in the torque equation and the nonlinear coupling between the rotor speed and the stator currents, the conventional PI controllers cannot offer stability and high precision on control. That's why, several nonlinear control techniques have been developed such as Sliding Mode Control (SMC) [5], and the Backstepping Control (BC) [6].

The first nonlinear control strategy treated in this paper is the backstepping control technique. The backstepping approach has been studied and developed to control the induction machines [7, 8] as well as the PMSG [9]. The basic idea of backstepping design is to select recursively some appropriate functions of state variables as pseudo control inputs for lower dimension subsystems of overall system. Each backstepping step is a new control inputs for the next step. All control stages are based on the *Lyapunov* theory [10]. The advantages of BC are reduced hardware complexity, reduced size of the drives and insensitivity to parameter variations. It offers high performances for trajectories tracking even with parameters variations [11].

The second nonlinear control strategy treated in this paper is the sliding mode control technique. This approach is commonly used due to its reliability, efficiency and insensitivity to parameters variations and external disturbances. Therefore, the stability of the system is proved by the *Lyapunov* algorithm [12, 13].

Both control strategies suppose that all state variables are available for feedback but the stator flux is inaccessible for measurements. Hence, the integration of a flux observer on the design control becomes unavoidable to make the stator flux known for feedback on one hand and to reduce the cost since there is no need to current sensors, on the other hand. Various research works have been devoted in this area. In this trend, the sliding mode flux observer is widely implemented [14] and it gives high robustness and stiffness under parameters variations. The backstepping flux observer (BFO) is one of the most efficient flux observers in the literature [15]. In fact, the observer based on the backstepping algorithm considers the prediction errors of the flux components as the state variables of the system with the aim of adjusting the tracking errors between the prediction errors and its references. The BFO takes into account parameter's variations, that's why the online estimation of the resistance is required to guarantee the stability of the whole system with the application of the *Lyapunov* theory [16].

In this paper we illustrate the effectiveness of the BFO inserted into nonlinear control strategies design of the wind generation system (WGS) based on the PMSG.

This paper is organized as follows: In second section, we present a modeling of a wind power generation system based on a PMSG. Third section deals with the development of the two nonlinear control strategies mentioned above for the stator side converter. In the fourth section, we study the two nonlinear control strategies applied to the grid side converter. Then the synthesis of the BFO with the estimation of the stator resistance is presented in section five. Two adaptive approaches are tested with dynamic simulation using Matlab/Simulink; the results are illustrated and discussed in section six.

2. Modeling of the Wind Generation System

The studied system is composed by three-bladed wind turbine, a PMSG, two power converters, a DC-link capacitor and a grid filter.
The stator of the generator is connected to grid through a full scale voltage source converter. Two control strategies are applied to the stator side converter (SSC) and the grid side converter (GSC). The first control approach is the BC, while the second one is SMC. The figure 1 presents the design of the WGS based on the PMSG.
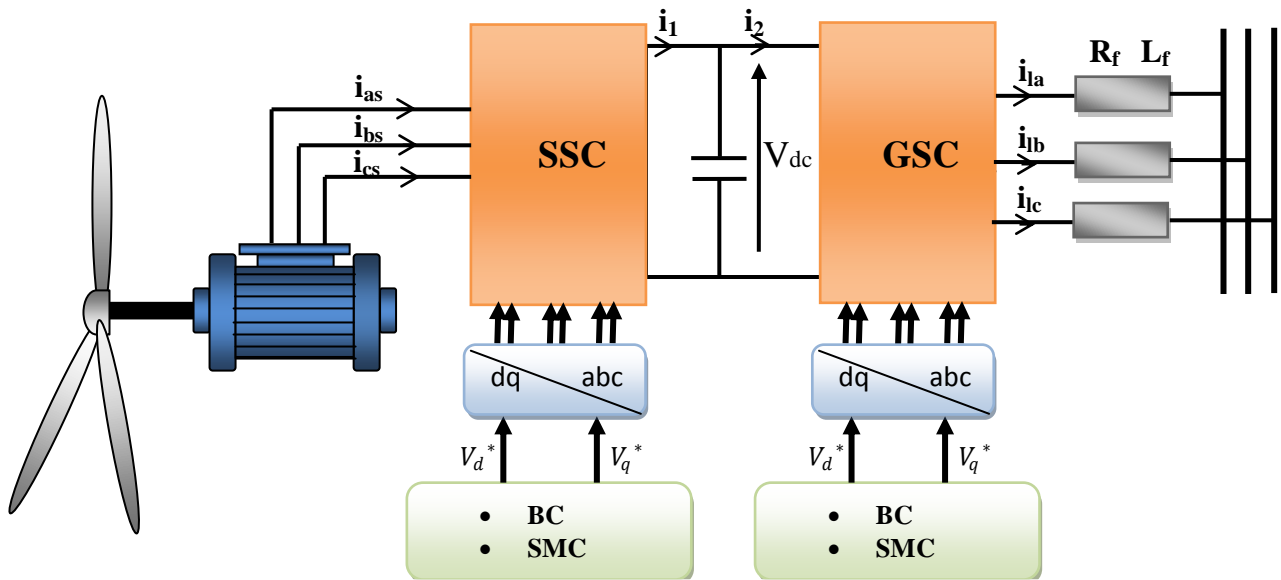
Figure 1: The structure of the wind energy conversion system based on a PMSG

2.1. PMSG Model

Taking into account the hypothesis commonly considered in AC machine modeling, electrical equations of the PMSG expressed in a (d, q) reference frame are given as [17]:

$$\begin{cases} v_d = R_s i_d + \dfrac{d\varphi_d}{dt} - \omega_r \varphi_q \\ v_q = R_s i_q + \dfrac{d\varphi_q}{dt} + \omega_r \varphi_d \end{cases} \tag{1}$$

The reference frame is linked to the rotor flux vector, so the stator flux components are expressed as:

$$\begin{cases} \varphi_d = L_d i_d + \varphi_r \\ \varphi_q = L_q i_q \end{cases} \tag{2}$$

The electromagnetic torque is linked to the currents by the expression (3):

$$T_{em} = \frac{3}{2} n_p (\varphi_r + (L_d - L_q) i_d) i_q \tag{3}$$

The stator active and reactive powers can be expressed as:

$$\begin{cases} P_s = \dfrac{3}{2}(v_d i_d + v_q i_q) \\ Q_s = \dfrac{3}{2}(v_q i_d - v_d i_q) \end{cases} \tag{4}$$

2.2. Turbine Model

The mechanical energy conversion system is described by the following equation:

$$T_m - T_{em} - K_f \Omega_r = J \frac{d\Omega_r}{dt} \tag{5}$$

The mechanical torque developed by a wind turbine is given as the following [18]:

$$T_m = \frac{1}{2} \rho \pi R^2 C_p \frac{V^3}{\Omega_r} \tag{6}$$

From the equation above, the power delivered from the wind turbine can be written

$$P_m = \frac{1}{2} \rho \pi R^2 C_p V^3 \tag{7}$$

3. Sator-side Converter Control

The SSC is controlled by two nonlinear control strategies; we present below the BC and then the SMC technique.

3.1. Backstepping Control Strategy

3.1.1. Description model

Taking into account equations (1), (2) and (5), the model of the system can be presented as:

$$\begin{cases} \dfrac{di_d}{dt} = \dfrac{1}{L_d}(-R_s i_d + n_p \Omega_r L_q i_q + v_d) \\[2mm] \dfrac{di_q}{dt} = \dfrac{1}{L_q}(-R_s i_q - n_p \Omega_r L_d i_d - n_p \Omega_r \varphi_r + v_d) \\[2mm] \dfrac{d\Omega_r}{dt} = \dfrac{1}{J}(T_m - T_{em} - K_f \Omega_r) \end{cases} \quad (8)$$

One can notice that the electromagnetic torque is directly proportional to the quadrature current component as long as the direct stator current component i_d is set to zero; furthermore the stator flux linkage φ_{ds} depends only on the rotor flux. As a result, the speed control can be achieved by controlling i_q.

In that way, the PMSG model can be expressed as [19]:

$$\begin{cases} v_d = -\omega_r L_q i_q \\[2mm] \dfrac{di_q}{dt} = \dfrac{1}{L_q}(-R_s i_q - \omega_r \varphi_r + v_q) \end{cases}$$

(9)

The expression (3) of the electromagnetic torque is reduced to:

$$T_{em} = \frac{3}{2} n_p \varphi_r i_q \quad (10)$$

3.1.2. BC Design

The basic idea of BC is to decompose the nonlinear control design problem into various design steps. Each step provides references for the next design step [20]. For the PMSG control design, the BC can be achieved by two successive steps.

- **Step1: Computation of the Reference Stator Currents**

The speed tracking error can be defined by:

$$e = \Omega_r^* - \Omega_r \quad (11)$$

The speed error dynamic can be presented as:

$$\dot{e} = \frac{1}{J}\left(-T_m + K_f \Omega_r + \frac{3}{2} n_p (\varphi_r + (L_d - L_q)i_d)i_q\right) \quad (12)$$

To reduce the speed tracking error to zero, current components are identified as the virtual control elements. Using the stability theory, the *Lyapunov* function is defined as:

$$V_1 = \frac{1}{2}e^2 \quad (13)$$

The derivative of equation (13) gives:

$$\dot{V}_1 = e\,\dot{e} = -K_s e^2 + \frac{e}{J}\left(-T_m + K_f \Omega_r + K_s Je + \frac{3}{2} n_p \varphi_r i_q\right)$$
$$+ \frac{3}{2J} n_p (L_d - L_q)i_d i_q e \quad (14)$$

where k_s is the speed closed loop feedback constant.

The *Lyapunov* function becomes $\dot{V}_1 = -k_s e^2 < 0$ if the current references are defined as:

$$\begin{cases} i_d^* = 0 \\[2mm] i_q^* = \dfrac{2}{3n_p \varphi_r}(T_m - K_f \Omega_r - K_s Je) \end{cases} \quad (15)$$

- **Step 2: Computation of the Reference Stator Voltages**

Let us consider the current tracking errors expressed as the following:

$$\begin{cases} e_d = i_d^* - i_d \\[2mm] e_q = i_q^* - i_q \end{cases} \quad (16)$$

Using equations (15) and (16), the equation (12) becomes:

$$\dot{e} = \frac{1}{J}\left(-K_s Je - \frac{3}{2} n_p \varphi_r e_q - \frac{3}{2} n_p (L_d - L_q)i_q e_d\right) \quad (17)$$

From equations (1), (10) and (11), the derivative of the current tracking errors can be expressed as:

$$\begin{cases} \dot{e}_d = \dfrac{1}{L_d}(R_s i_d - \omega_r L_q i_q - v_d) \\[2mm] \dot{e}_q = \dfrac{2}{3Jn_p \varphi_r}(JK_s - K_f)(T_m - K_f \Omega_r - \dfrac{3}{2} n_p \varphi_r i_q \\[2mm] \quad - \dfrac{3}{2} n_p (L_d - L_q)i_d i_q) + \dfrac{1}{L_q}(R_s i_q + \omega_r L_d i_d + \omega_r \varphi_r - v_q) \end{cases} \quad (18)$$

To determine the stator voltage references, a new *Lyapunov* function based on the speed tracking error and current components errors is defined:

$$V_2 = \frac{1}{2}e^2 + \frac{1}{2}e_d^2 + \frac{1}{2}e_q^2 \quad (19)$$

By differentiating the second *Lyapunov* function, one easily obtains:

$$V_2 = e\,\dot{e} + e_d\,\dot{e}_d + e_q\,\dot{e}_q \tag{20}$$

By substituting equations (17) and (18) on the equation (20) the derivative can be expressed as the following:

$$\dot{V}_2 = A + B \tag{21}$$

with:

$$
\begin{cases}
A = -k_s e^2 - k_1 e_d^2 - k_2 e_q^2 \\[2mm]
B = \dfrac{e}{J}\left[-\dfrac{3}{2}n_p\varphi_r e_q - \dfrac{3}{2}n_p\left(L_d - L_q\right)e_d i_q \right] \\[3mm]
+ \dfrac{e_d}{L_d}\left[R_s i_d - \omega_r L_q i_q + k_1 L_d e_d - v_d \right] + \dfrac{e_q}{L_q}\left[\dfrac{2L_q}{3Jn_p\varphi_r}\left(Jk_s - K_f\right)\right. \\[3mm]
\left(T_m - \dfrac{3}{2}n_p\varphi_r i_q - \dfrac{3}{2}n_p\left(L_d - L_q\right)i_d i_q - K_f\Omega_r\right) \\[3mm]
\left.+ R_s i_q + \omega_r L_d i_d + \omega_r\varphi_r + k_2 L_q e_q - v_q\right]
\end{cases} \tag{22}
$$

The derivative of the *Lyapunov* function is considered definite negative if $\dot{V}_2 < 0$, then B converges to zero. We obtain:

$$
\begin{cases}
\dot{V}_2 = A < 0 \\
B = 0
\end{cases} \tag{23}
$$

Thus, one can easily obtain the following d-q voltage references:

$$
\begin{cases}
v_d^* = R_s i_d - \omega_r L_q i_q + k_1 L_d e_d + \dfrac{3}{2J}n_p L_d (L_d - L_q)i_q e \\[3mm]
v_q^* = R_s i_q + \omega_r L_d i_d + \omega_r\varphi_r + \dfrac{2L_q}{3Jn_p\varphi_r}(Jk_s - K_f) \\[3mm]
\left(T_m - K_f\Omega_r - \dfrac{3}{2}n_p\varphi_r i_q - \dfrac{3}{2}n_p(L_d - L_q)i_d i_q\right) \\[3mm]
- \dfrac{3}{2J}n_p\varphi_r L_q e + k_2 L_q e_q
\end{cases} \tag{24}
$$

Where k_1 and k_2 are positive parameters selected to stabilize the system.

3.2. Sliding Mode Control Strategy

The SMC design is based on the selection of the sliding surface and the control of system variables in order to reach the selected surface since the *Lyapunov* stability algorithm was verified.

3.2.1. Description model

The non-linear system can be presented by the following state model [21]:

$$\dot{x}(t) = f(t,x) + g(t,x)u(t) \tag{25}$$

The state model of our system is given as :

$$
\begin{cases}
\dfrac{d\Omega_r}{dt} = \dfrac{1}{J}(T_m - T_{em} - K_f\Omega_r) \\[3mm]
\dfrac{di_q}{dt} = \dfrac{1}{L_q}(-R_s i_q - n_p\Omega_r L_d i_d - n_p\Omega_r\varphi_r + v_q) \\[3mm]
\dfrac{di_d}{dt} = \dfrac{1}{L_d}(-R_s i_d + n_p\Omega_r L_q i_q + v_d)
\end{cases} \tag{26}
$$

From the model mentioned above, one can easily conclude that:

$$
x(t) = \begin{pmatrix} \Omega_r \\ i_q \\ i_d \end{pmatrix}, \quad u(t) = \begin{pmatrix} v_q \\ v_d \end{pmatrix}, \quad g(t,x) = \begin{pmatrix} 0 & 0 \\ \dfrac{1}{L_q} & 0 \\ 0 & \dfrac{1}{L_d} \end{pmatrix} \text{ and}
$$

$$
f(t,x) = \begin{pmatrix} \dfrac{1}{J}(T_m - T_{em} - K_f\Omega_r) \\[3mm] \dfrac{1}{L_q}(-R_s i_q - n_p\Omega_r L_d i_d - n_p\Omega_r\varphi_r) \\[3mm] \dfrac{1}{L_d}(-R_s i_d + n_p\Omega_r L_q i_q) \end{pmatrix}
$$

3.2.2. Control Design

We have defined three sliding surfaces: the first one is for the speed, the second one is for the quadrature current component and the third one is for the direct current component.

The sliding surface $S(x_i)$ is the error between the reference value and the actual value of the state variable such as:

$$
\begin{cases}
S(\Omega_r) = \Omega_r^* - \Omega_r \\
S(i_q) = i_q^* - i_q \\
S(i_d) = i_d^* - i_d
\end{cases} \tag{27}
$$

The adopted control law is composed of two terms; one is a continuous term u_{ieq} and the other is a discontinuous term:

$$u_i = u_{ieq} + u_{iN} \tag{28}$$

where u_{ieq} is the i-th component of the equivalent control who guarantees $\dot{S}(x_i) = 0$ and where u_{iN} depends on the sign of the sliding surface.

$$u_{ieq} = -\left[\frac{\partial S(x_i)}{\partial x_i}.g(x,t)\right]^{-1}\left[\frac{\partial S(x_i)}{\partial x}.f(x,t)\right] \quad (29)$$

$$u_{iN} = K_i.sign(S(x_i)) \quad (30)$$

where K_i is a constant positive gain.

During this mode of control, the *Lyapunov* condition must be verified: the product of the surface with its derivative must be less than zero [22]:

$$S(x_i).\dot{S}(x_i) < 0 \quad (31)$$

Using equations (27) and (29), the vector of the equivalent control is given by:

$$U_{eq} = \begin{pmatrix} i_{qeq} \\ v_{qeq} \\ v_{deq} \end{pmatrix} = \begin{pmatrix} \dfrac{(K_f\Omega_r - T_m)}{-n_p(\varphi_r - (L_d - L_q)i_d)} \\ R_s i_q + n_p\Omega_r L_d i_d + n_p\Omega_r\varphi_r \\ R_s i_d - n_p\Omega_r L_q i_q \end{pmatrix} \quad (32)$$

The vector of the discontinuous term is defined as:

$$U_N = \begin{pmatrix} i_{qN} \\ v_{qN} \\ v_{dN} \end{pmatrix} = \begin{pmatrix} K_\Omega sign(S(\Omega_r)) \\ K_q sign(S(i_q)) \\ K_d sign(S(i_d)) \end{pmatrix} \quad (33)$$

As a result, we obtain:

$$\begin{cases} i_q^* = i_{qeq} + i_{qN} \\ v_q^* = v_{qeq} + v_{qN} \\ v_d^* = v_{deq} + v_{dN} \end{cases} \quad (34)$$

4. Grid-side converter Control

The GSC is connected to the grid by an intermediary line characterized by a resistance R_f and an inductance L_f. It controls the power delivered to the grid.

For the GSC, we present two control strategies. The first approach is the BC; the second one is the SMC strategy.

4.1. Backstepping Control Strategy

4.1.1 Model description

The grid-side equations are expressed in the (d, q) reference frame as [23]:

$$\begin{cases} \dfrac{di_{ld}}{dt} = \dfrac{v_{ld}}{L_f} - \dfrac{R_f}{L_f}i_{ld} + \omega_g i_{lq} \\ \dfrac{di_{lq}}{dt} = \dfrac{v_{lq}}{L_f} - \dfrac{R_f}{L_f}i_{lq} - \omega_g i_{ld} + v_g \end{cases} \quad (35)$$

where ω_g is the grid pulsation and v_g is the grid voltage amplitude.

The active and the reactive powers are linked to the current components by the following expressions:

$$\begin{cases} P = \dfrac{3}{2}(v_{gd}i_{ld} + v_{gq}i_{lq}) \\ Q = \dfrac{3}{2}(v_{gq}i_{ld} - v_{gd}i_{lq}) \end{cases} \quad (36)$$

In this session, we adopt the conditions of the vector control strategy; thus, the direct axis of the reference frame is oriented to the grid voltage vector. We obtain: $v_{gq} = 0$.

As a result, equation (36) becomes:

$$\begin{cases} P = \dfrac{3}{2}v_{gd}i_{ld} \\ Q = -\dfrac{3}{2}v_{gd}i_{lq} \end{cases} \quad (37)$$

One can easily conclude that power dynamics depend only on current components control.

4.1.2 Control design

The grid current errors are defined as:

$$\begin{cases} e_{ld} = i_{ld}^* - i_{ld} \\ e_{lq} = i_{lq}^* - i_{lq} \end{cases} \quad (38)$$

The derivative of the above equations gives:

$$\begin{cases} \dot{e}_{ld} = -\dot{i}_{ld} \\ \dot{e}_{lq} = -\dot{i}_{lq} \end{cases} \quad (39)$$

In order to generate the references of line voltages, we have to define the *Lyapunov* function related to the grid current errors. It can be written as:

$$V_3 = \frac{1}{2}(e_{ld}^2 + e_{lq}^2) \quad (40)$$

Referring to (35) and (39), the derivative of (40) is expressed as:

$$\dot{V}_3 = -k_{ld}e_{ld}^2 - k_{lq}e_{lq}^2 + e_1(\frac{v_{ld}}{L_f} - \frac{R_f}{L_f}i_{ld} + \omega_g i_{lq} + k_{ld}e_{ld})$$

$$+ e_2(\frac{v_{lq}}{L_f} - \frac{R_f}{L_f}i_{lq} - \frac{v_g}{L_f} - \omega_g i_{ld} + k_{lq}e_{lq}) \tag{41}$$

To insure the condition that the derivative of the *Lyapunov* function is negative $\dot{V}_3 < 0$, the following conditions should be verified:

$$\begin{cases} v_{ld}^* = R_f i_{ld} - L_f \omega_g i_{lq} - L_f k_{ld}e_{ld} \\ v_{lq}^* = R_f i_{lq} + L_f \omega_g i_{ld} - L_f k_{lq}e_{lq} + v_g \\ k_{ld} > 0 \\ k_{lq} > 0 \end{cases} \tag{42}$$

such as k_{ld} and k_{lq} are constant gains.

After satisfying conditions mentioned above, the derivative of the *Lyapunov* function becomes:

$$\dot{V}_3 = -k_{ld}e_{ld}^2 - k_{lq}e_{lq}^2 < 0 \tag{43}$$

4.2. SMC Strategy

The same model presented on (35) is adopted in this section. The two sliding surfaces referred to grid current components are defined as:

$$\begin{cases} S(i_{ld}) = i_{ld}^* - i_{ld} \\ S(i_{lq}) = i_{lq}^* - i_{lq} \end{cases} \tag{44}$$

Using equation (29), the equivalent control components are written as:

$$\begin{cases} v_{ld-eq} = R_f i_{ld}^* - \omega_g i_{lq}^* \\ v_{lq-eq} = R_f i_{lq}^* + \omega_g i_{ld}^* \end{cases} \tag{45}$$

The discontinuous terms of this control are defined by the following:

$$\begin{cases} v_{ld-N} = k_{ld}sign(S(i_{ld})) \\ v_{lq-N} = k_{lq}sign(S(i_{lq})) \end{cases} \tag{46}$$

As a result, the line voltage reference is the sum of the two terms expressed in (45) and (46):

$$\begin{cases} v_{ld}^* = R_f i_{ld}^* - \omega_g i_{lq}^* + k_{ld}sign(S(i_{ld})) \\ v_{lq}^* = R_f i_{lq}^* + \omega_g i_{ld}^* + k_{lq}sign(S(i_{lq})) \end{cases} \tag{47}$$

From (36), one can deduce the expressions of current references:

$$\begin{cases} i_{ld}^* = \frac{P^* v_{gd} + Q^* v_{gq}}{v_{gd}^2 + v_{gq}^2} \\ i_{lq}^* = \frac{P^* v_{gq} - Q^* v_{gd}}{v_{gd}^2 + v_{gq}^2} \end{cases} \tag{48}$$

where P^* and Q^* are the reference of the active power transported to the grid and the reference of the reactive power received from the grid, respectively.

We have to know that the active power transported to the grid is given by:

$$P = V_{DC}i_1 - V_{DC}i_c \tag{49}$$

such as the DC bus voltage can be expressed as follows:

$$V_{DC} = \frac{1}{C}\int i_c dt$$

(50)

where i_c is the DC bus current and i_l is the modulated current from the stator side converter.

5. An Adaptive Backstepping Flux Observer

The BC and the SMC strategies consider that all PMSG variables are known, but the stator flux is inaccessible for measurement. That's why a BFO is proposed to calculate the stator flux components.

Only the stator flux and the stator resistance are replaced by their values created by the BFO.

Using the equation (2), one can conclude that stator flux components depend directly on stator current components. Consequently, the flux observation requires the observation of the stator current components.

The BFO can be formulated as [24]:

$$\begin{cases} \frac{d\hat{i}_d}{dt} = \frac{1}{L_d}(-\hat{R}_s\hat{i}_d + n_p\Omega_r L_q \hat{i}_q + v_d) + u_d \\ \frac{d\hat{i}_q}{dt} = \frac{1}{L_q}(-\hat{R}_s\hat{i}_q - n_p\Omega_r L_d \hat{i}_d - n_p\Omega_r\varphi_r + v_d) + u_q \end{cases} \tag{51}$$

where $\hat{x}$ is the estimation of the variable x and the estimated resistance is written as: $R_s = \hat{R}_s + \Delta R_s$.

u_d and u_q are the control inputs of the BFO.

The state errors can be defined as follows:

$$\begin{cases} e_1 = i_d - \hat{i}_d \\ e_2 = i_q - \hat{i}_q \end{cases} \tag{52}$$

920

where e_1 and e_2 are the stator current observer errors. The prediction errors dynamic is given by the following equation:

$$\begin{cases} \dot{e}_1 = \dfrac{-R_s}{L_d} e_1 + \dfrac{n_p \Omega_r L_q}{L_d} e_2 - \dfrac{\Delta R_s}{L_d} \hat{i}_d - u_1 \\ \dot{e}_2 = \dfrac{-R_s}{L_q} e_2 - \dfrac{n_p \Omega_r L_d}{L_q} e_1 - \dfrac{\Delta R_s}{L_q} \hat{i}_q - u_2 \end{cases} \qquad (53)$$

5.1. BFO Design

The observer is based on the backstepping technique, thus it is accomplished by two steps.

- **Step1**

We define the integral of the currents prediction errors as follows [25]:

$$\begin{cases} \dot{e}_\alpha = e_1 \\ \dot{e}_\beta = e_2 \end{cases} \qquad (54)$$

e_1 , e_2 are virtual control variables of the BFO with y_1 , y_2 are its reference trajectories.
Then, the tracking errors of the prediction errors are expressed as follows:

$$\begin{cases} z_1 = e_1 - y_1 \\ z_2 = e_2 - y_2 \end{cases} \qquad (55)$$

The observer's dynamics are based on the exponential convergence, so that the expressions of the references of the prediction errors are written as:

$$\begin{cases} y_1 = -\lambda_1 e_\alpha \\ y_2 = -\lambda_1 e_\beta \end{cases} \qquad (56)$$

- **Step2**

Substituting equation (56) on equation (55), we obtain:

$$\begin{cases} z_1 = e_1 + \lambda_1 e_\alpha \\ z_2 = e_2 + \lambda_1 e_\beta \end{cases} \qquad (57)$$

Using equations (53), (54) and (57), the control inputs are expressed by the following:

$$\begin{cases} u_1 = \dfrac{L_q}{L_d} n_p \Omega_r e_2 + \lambda_1 e_1 + \lambda_2 z_1 + e_\alpha \\ u_2 = -\dfrac{L_d}{L_q} n_p \Omega_r e_1 + \lambda_1 e_2 + \lambda_2 z_2 + e_\beta \end{cases} \qquad (58)$$

and:

$$\begin{cases} \dot{z}_1 = \dfrac{-R_s}{L_d} e_1 - \dfrac{\Delta R_s}{L_d} \hat{i}_d - \lambda_2 z_1 - e_\alpha \\ \dot{z}_2 = \dfrac{-R_s}{L_q} e_2 - \dfrac{\Delta R_s}{L_q} \hat{i}_q - \lambda_2 z_2 - e_\beta \end{cases} \qquad (59)$$

5.2. Stator Resistance Estimation

The BFO takes into account the variations of the stator resistance, so that, this latter has been estimated via the *Lyapunov* function written as [26]:

$$V_e = \frac{1}{2}(e_\alpha^2 + e_\beta^2 + z_1^2 + z_2^2 + \frac{\Delta R_s^2}{q}) \qquad (60)$$

where q is a constant positive gain
The derivative of the *Lyapunov* function is given by:

$$\dot{V}_e = e_\alpha \dot{e}_\alpha + e_\beta \dot{e}_\beta + z_1 \dot{z}_1 + z_2 \dot{z}_2 + \frac{\Delta R_s}{q} \frac{d\Delta R_s}{dt} \qquad (61)$$

To satisfy the *Lyapunov* condition and make the function definite negative, we have to adjust the expression of the stator resistance adaptation as follows:

$$\frac{d\hat{R}_s}{dt} = q(\frac{\hat{i}_d}{L_d} z_1 + \frac{\hat{i}_q}{L_q} z_2) \qquad (62)$$

The stator resistance variations are presented in figure 2.
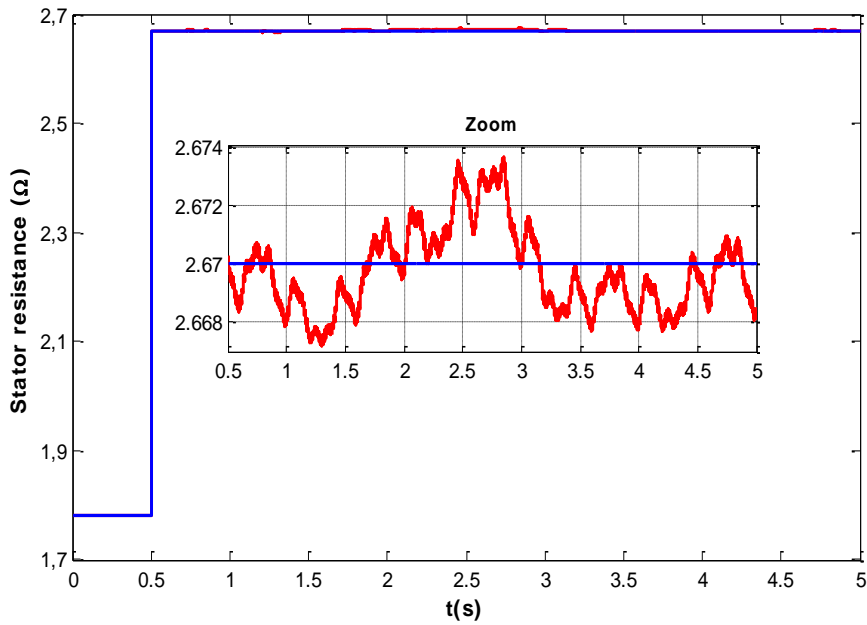
Figure 2: Stator resistance variations

Figure 3 shows the bloc diagram of the proposed control strategy- BFO applied to the PMSG.
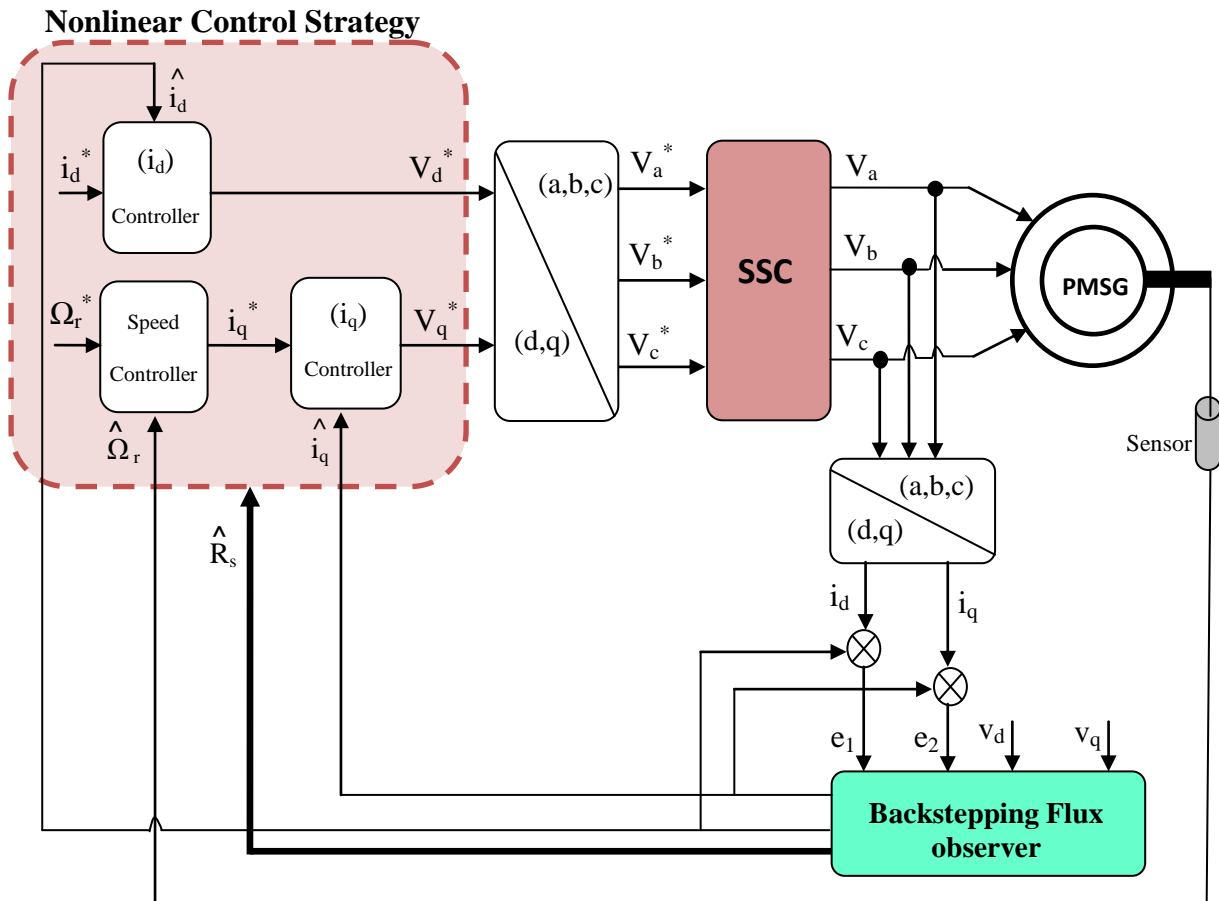

Figure 3: Bloc Diagram of the proposed SSC control strategy-BFO applied to the PMSG

6. Simulation results

The overall WGS design shown above is implemented on the MATLAB interface and it's simulated to confirm the validity and the reliability of both nonlinear control strategies applied to the SSC and the GSC with an adaptive BFO. Simulations are carried out, with a generator rated at 5kW, to make a comparative study between the two control techniques and to investigate performances offered by the observer.

All simulation's studies are achieved with the same DC bus voltage equal to 790V and the same wind speed modeling as the following sinusoidal function:

$$V=7+ \sin(\frac{2\pi}{7}t)-0.875 \sin(\frac{6\pi}{7}t)+ 0.75\sin(\frac{10\pi}{7}t)$$
$$-0.625 \sin(\frac{20\pi}{7}t)+0.5\sin(\frac{60\pi}{7}t)+0.25\sin(\frac{100\pi}{7}t)+0.125 \tag{63}$$

The wind profile represented in the figure 4 show two velocity peaks; the first peak registered at 1.9s, the second one at 5.1s.
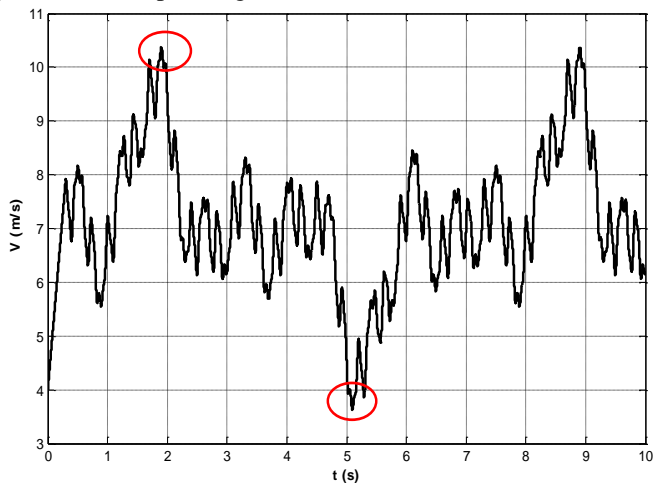

Figure 4: Wind speed profile

Therefore, we have registered the WGS response to the combination of the two control strategies applied to the SSC as well as to the GSC. All combination cases are illustrated in the table 1.

Table 1: Different combination of the control strategies applied to the SSC and the GSC

	Case n°1	Case n°2	Case n°3	Case n°4
SSC	BC	BC	SMC	SMC
GSC	SMC	BC	BC	SMC

Firstly, we focus on the response time of the rotor speed, the stator flux and the torque as presented in the table 2. One can easily conclude that the speed, torque and flux have quick responses when the two converters are controlled by the same BC strategy (case n°2).

Table 2: The response time of each variable for all possible combinations

	Case n°1	Case n°2	Case n°3	Case n°4
$t_{r\_\Omega_r}(s)$	0.025	0.02	0.027	0.05
$t_{r\_\varphi_s}(s)$	0.036	0.025	0.06	0.05
$t_{r\_T_{em}}(s)$	0.019	0.008	0.03	0.05

Secondly, we investigate, in the table 3, relative errors of the same variables in different cases of control. In fact, errors of the speed, flux and torque are defined at two different times of peak (at t=1.9s and t=5.1s). Generally, the error of a variable "x" is given by the following expression:

$$e_x(\%) = 100\frac{x^* - x}{x^*} \tag{64}$$

In our study, "x" is the estimated variable generated by the BFO.

Table 3: Summarization of relative errors of speed, flux and torque

		Case n°1	Case n°2	Case n°3	Case n°4
$e_{\Omega_r}(\%)$	t=1.9s	0.05	0.05	0.66	0.65
	t=5.1s	0.12	0.1	0.425	0.4
$e_{\varphi_s}(\%)$	t=1.9s	0.077	0.068	0.46	0.47
	t=5.1s	0.031	0.012	0.22	0.0025
$e_{T_{em}}(\%)$	t=1.9s	2.117	2.3	1.8	0.7
	t=5.1s	3.04	3.3	0.3	4.1

From table 3, we can conclude that all errors of the speed and the flux are small especially in the case n°2, however the torque error is the lowest in the case n°3 when the SSC is controlled by the SMC and the GSC is controlled by the BC. So that, table 2 and 3 show high performance in precision, tracking and robustness of the WGS based on the PMSG under SMC/BC and also BC/BC strategies.

Subsequently, we present responses of the rotational speed, the electromagnetic torque, the stator flux, the DC bus voltage and the stator active power in the figures 5, 6, 7, 8 and 9 respectively. As shown in these figures, all estimated variables follow its references trajectories perfectly even with several fluctuations of the wind allowing small tracking errors.

The mechanical speed, illustrated by the figure 5, records a low value when the wind speed is decreased at t=5.1s which confirms the correspondence between the rotational speed and the wind speed.

In addition, one can notice that the electromagnetic torque is affected by the fluctuations of the wind speed as shown in the figure 6. It has a few oscillations at the starting phase under SMC/BC and SMC/SMC strategies (fig.6 (c) and (d)) which retarded the tracking of the reference trajectory, that agree with values of the response time checked in the table 2. The same remarks are for the stator flux presented by the figure 7.

The Figure 8 shows the DC bus voltage profile, it converges rapidly to its reference value at 0.02s. It can be seen that the BC strategy offers better results when applied on the GSC.

Also, the stator active power is affected by the variations of the wind speed as investigated in the figure 9. Indeed, one can notice that the active power reaches high values with the SMC applied to the SSC.

According to the simulation results and tables mentioned above, we can confirm that the BFO offers good results in terms of reliability and efficiency on one hand, on the other hand we notice that the cases of control BC/BC and SMC/BC are more suitable for the WGS.

But owing to oscillations of the control variables illustrated at the starting phase in case of SMC/BC, we can conclude that the BC strategy is more appropriate to control the converters.

Finally, in order to exhibit good results obtained with the BFO, we have studied the WGS response under the proposed control strategy BC/BC with stator resistance variations. We have introduced a sudden increase of the stator resistance at t=0.5s. The corresponding simulation results are presented in figure 10.

Hence, as shown in figure 10 (a), few variations can be seen in the rotational speed profile when the resistance is increased at t=0.5s. The zoom of the electromagnetic torque presented in figure 10 (b) prove the rigidity of the control strategy, in fact within the resistance increase, the torque has overshoots to the normal profile but it returns after about 1s and follows its normal trajectory. In addition, the stator flux is insensitive to the resistance variations as seen in the figure 10 (c); the flux tracks its reference trajectory with a few oscillations not affecting the system control. As a review, the BC strategy with the BFO is characterized by its robustness against stator resistance variations proving the stability of overall system.
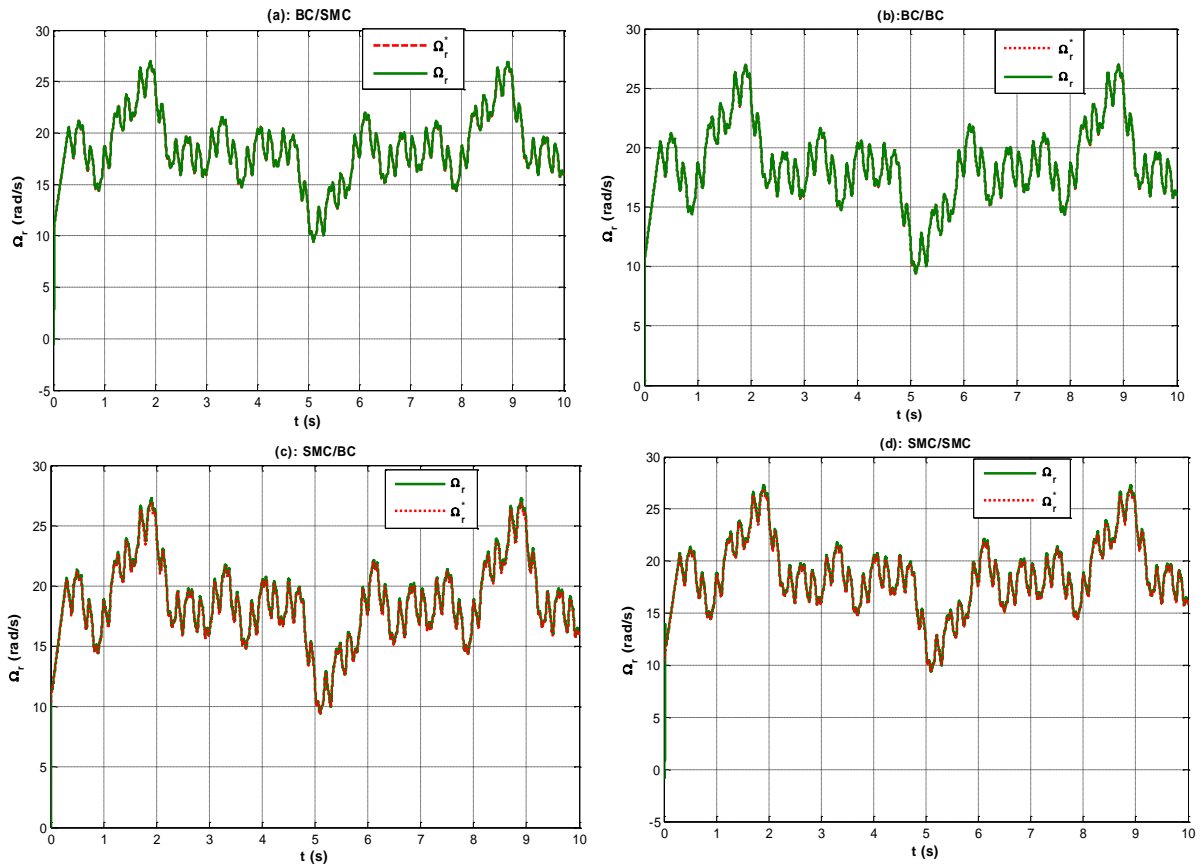
Figure 5: Simulation results: Rotational speed profile under all control strategies,
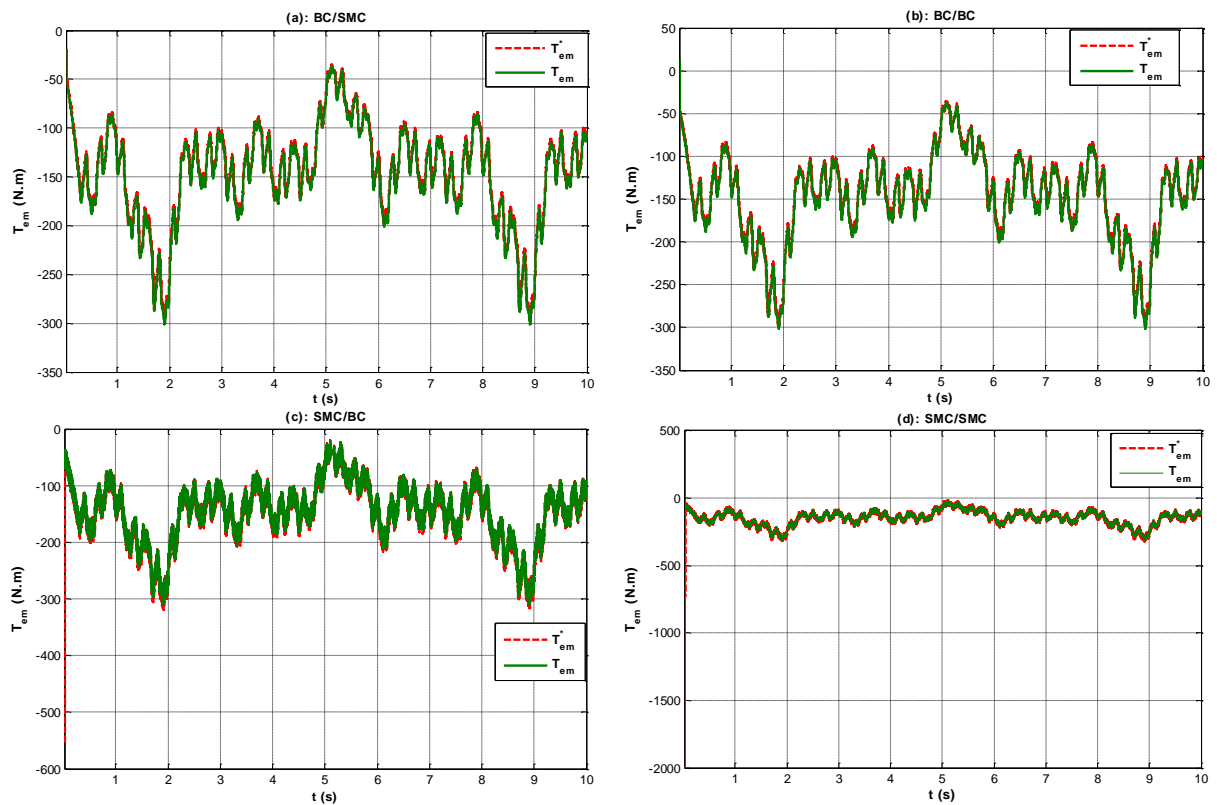Legend: (a) BC/SMC, (b) BC/BC, (c) SMC/BC, (d) SMC/SMC

Figure 6: Simulation results: Electromagnetic torque profile under all control strategies,
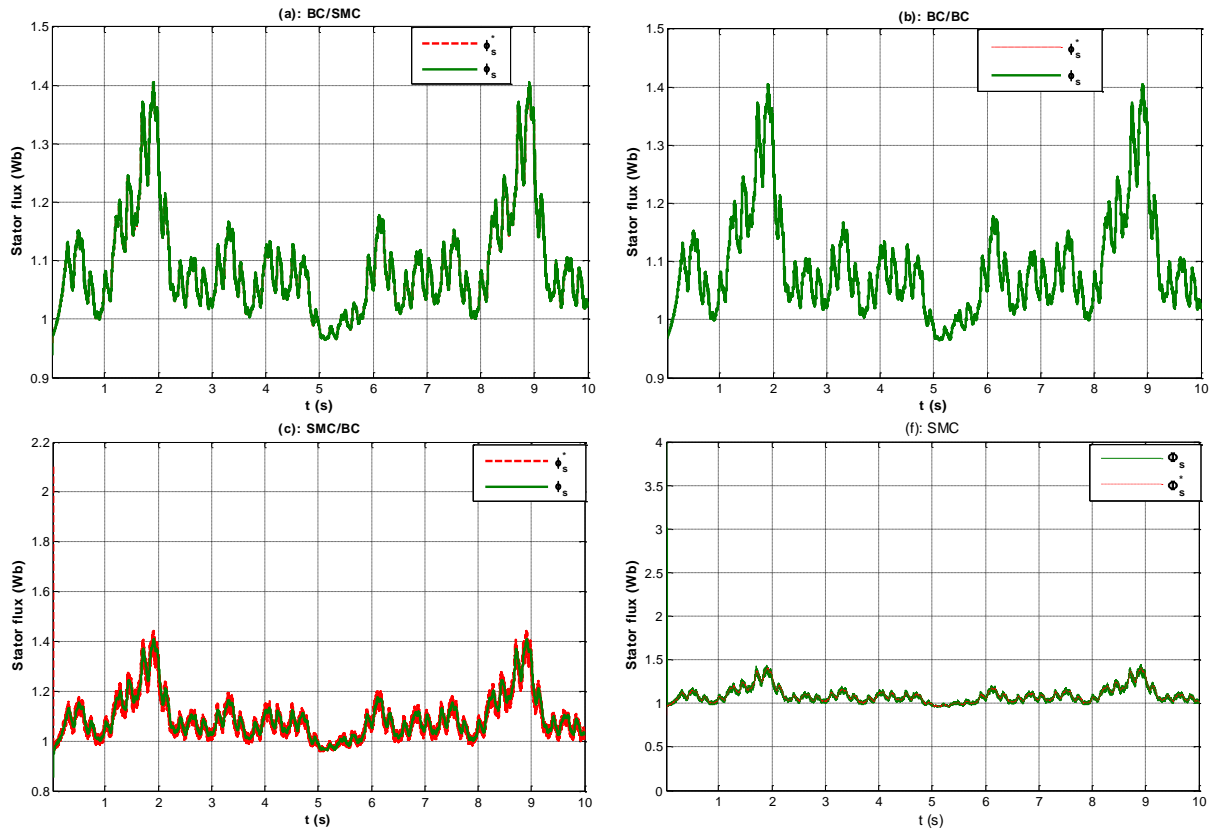Legend: (a) BC/SMC, (b) BC/BC, (c) SMC/BC, (d) SMC/SMC

Figure 7: Simulation results: Stator flux profile under all control strategies,
Legend: (a) BC/SMC, (b) BC/BC, (c) SMC/BC, (d) SMC/SMC
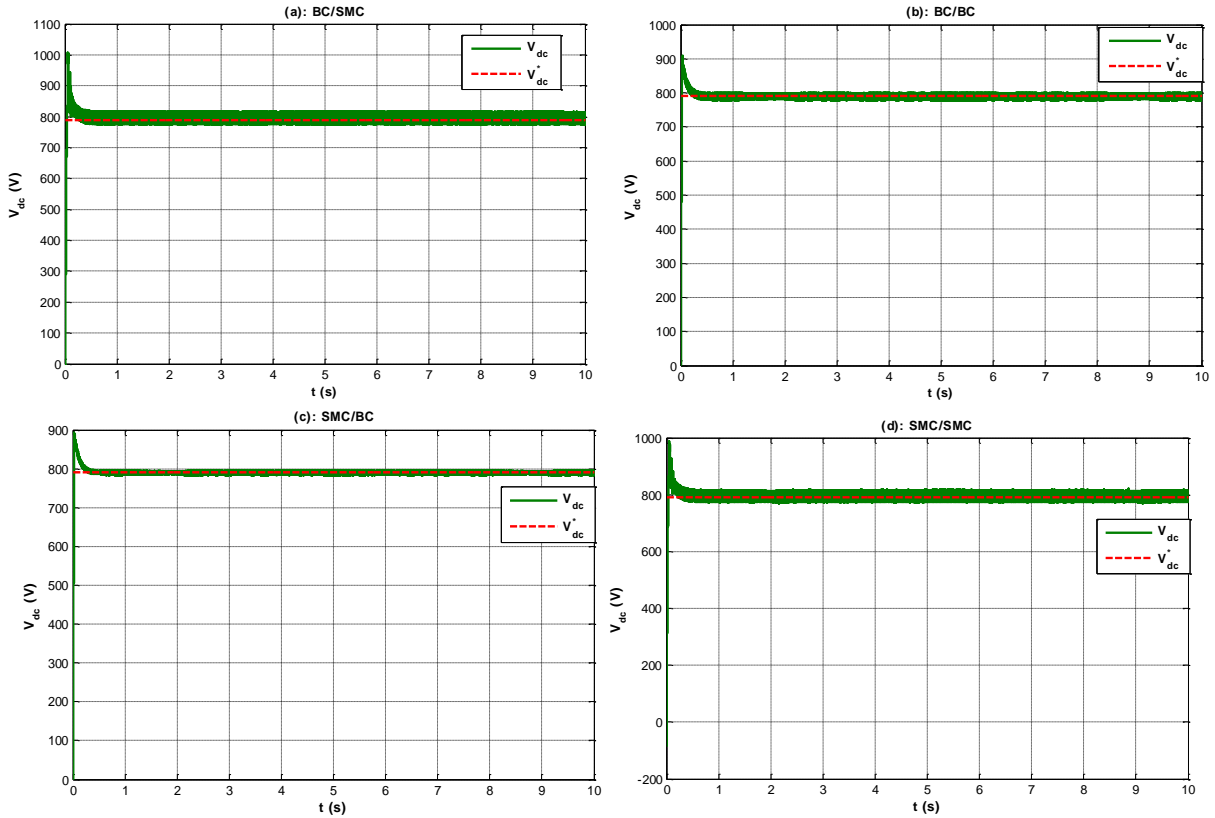

Figure 8: Simulation results: DC bus voltage profile under all control strategies,
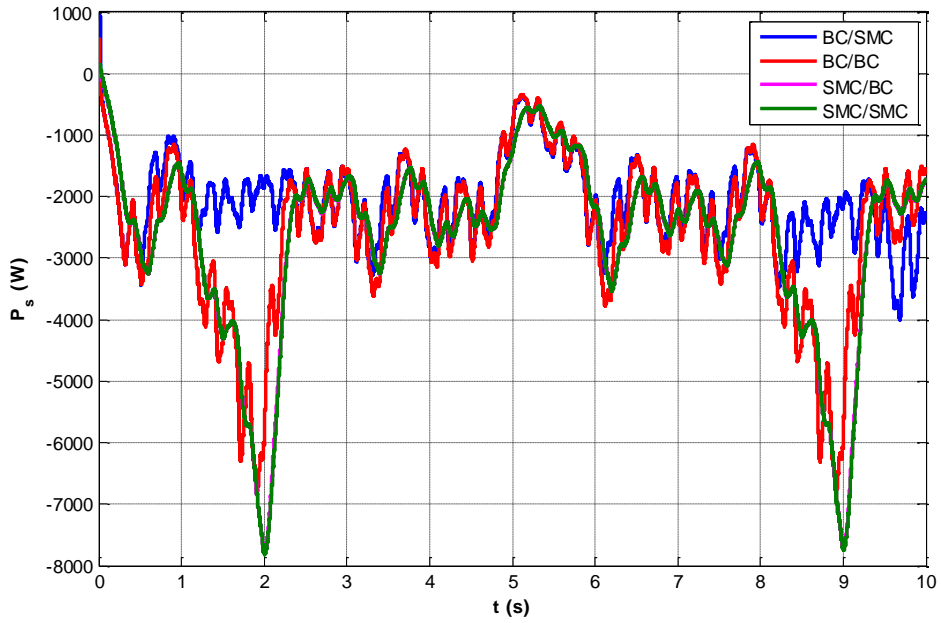Legend: (a) BC/SMC, (b) BC/BC, (c) SMC/BC, (d) SMC/SMC

Figure 9: Simulation results: Stator active power profile under all control strategies
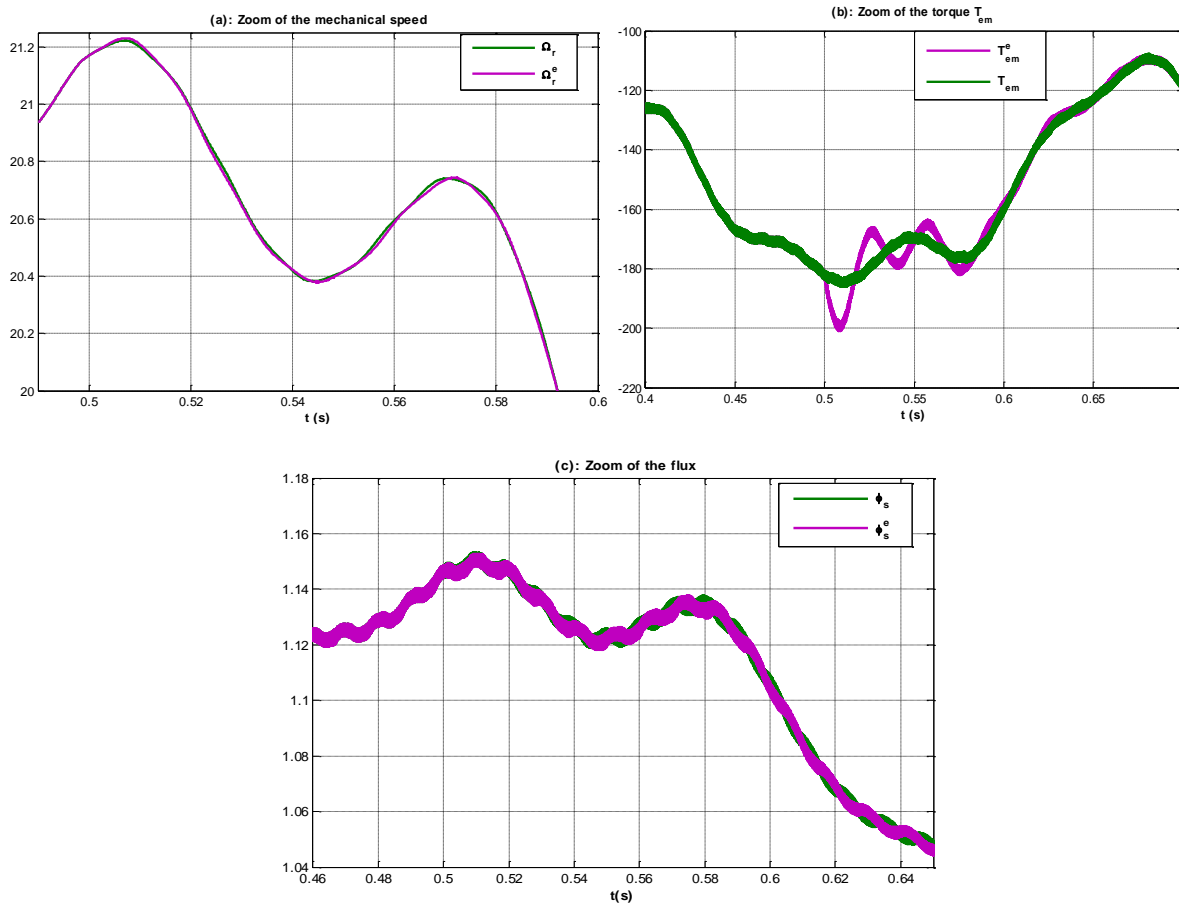

Figure 10: Simulation results of the BC/BC strategy under stator resistance variations
Legend: (a) zoom of the speed, (b) zoom of the torque, (c) zoom of the flux

7. Conclusion

The present paper presents an adaptive backstepping flux observer for two control strategies applied to the WGS based on the PMSG. The two control techniques designed to control both the converters are the backstepping control strategy and the sliding mode control one. Different combinations of control of the SSC/GSC are studied and compared: BC/SMC, BC/BC, SMC/BC and SMC/SMC. Despite the consecutive fluctuations of the wind speed, all cases of control present high dynamic performances in tracking and precision. According to simulation results, the backstepping control strategy, applied to the SSC as well as the GSC, is the most appropriate approach for the WGS based on the PMSG. Then in order to investigate the impact of the parameter variations, we introduced a sudden increase of the stator resistance. Thus, results show perfect tracking responses and robust characteristics against stator resistance variations.

Appendix

PMSG data	
Rated power	5kW
Rated stator voltage	550 V
Nominal frequency	50 Hz
Pole pairs number	n_p=10
Stator resistance	r_s =1.78Ω
Direct inductance	L_d =34.2mH
quadrature inductance	L_q =48.5mH
Rated torque	156 N.m
Rotor flux	φ_r =0.9566 Wb
Rated rotational speed	314 rad/s
Moment of inertia	J = 0.1 kg/m^2
Wind Turbine data	
Rated power	5kW
Blade radius	R_t = 2.7m
Power coefficient	C_{pmax} = 0.45
Optimal relative wind speed	λ_{opt}=9
Damping coefficient	K_f = 0.2

References

[1] E. Mahersi, A. Kheder and M.F. Mimouni, "The Wind energy conversion system using PMSG controlled by vector control and SMC strategies", *International Journal of Renewable Energy Research, Vol.3, N°.1, 2013.*

[2] S. Ladide, H. Hihi and AH. Khalid Fait, "Modeling and control of a permanent magnet Synchronous generator driven by a wind turbine", 2nd International Conference of Renewable Energies CIER-2014 Proceedings of Engineering and Technology - PET Copyright - IPCO 2015.

[3] X. Dominguez and C. Imbaquingo, "Vector control for an interior permanent magnet synchronous machine with maximum torque per ampere strategy", Revista Politécnica, Vol.35, N°. 1, pp: 1-5, April 2015.

[4] E. Mahersi, A. Kheder and M.F. Mimouni, "An adaptive sliding mode flux observer applied to wind PMSG system controlled by VC and SMC," Eighth International Conference and Exhibition on Ecological Vehicles and Renewable Energies (EVER), 2013, Monaco.

[5] X. Zhang, L. Sun, Ke Zhao and Li Sun, "Nonlinear Speed Control for PMSM System Using Sliding-Mode Control and Disturbance Compensation Techniques", IEEE Transactions on Power Electronics ,Vol.28 , N°.3.

[6] C. Chen, Y. Xie and Y. Lan, "Backstepping Control of Speed Sensorless Permanent Magnet Synchronous Motor Based on Slide Model Observer", International Journal of Automation and Computing 12(2), pp. 149-155, April 2015.

[7] R.Trabelsi, A.Khedher, M.F. Mimouni, F.M'Sahli and A.Masmoudi, "Rotor Flux Estimation Based on Nonlinear Feedback Integrator for Backstepping-Controlled Induction Motor Drives", Electromotion Journal 17, 2010, pp:163-172.

[8] N. Khemiri, A. Kheder, M.F. Mimouni, "An adaptive nonlinear backstepping control of DFIG driven by wind turbine", WSEAS Transactions on Environment and Development, N° 2, Vol.8, April 2012.

[9] A. Lagrioui, 2H. Mahmoudi, "Nonlinear adaptive backstepping control of permanent magnet synchronous motor (PMSM)", Journal of Theoretical and Applied Information Technology 15th July 2011. Vol. 29 N°.1. 2011.

[10] E. Mahersi and A. Kheder, "Adaptive Backstepping Control Applied to Wind PMSG System", The 7th International Renewable Energy Congress March 22-24, 2016 Hammamet, Tunisia.

[11] M. Morawiec, "The Adaptive Backstepping Control of Permanent Magnet Synchronous Motor Supplied by Current Source Inverter", IEEE Transactions on Industrial Informatics Vol.9 , N°. 2, pp: 1047 – 1055.

[12] E. Mahersi and A. Kheder, "Sensorless control with an adaptive sliding mode flux observer applied to wind PMSG system", 15th International Conference on Sciences and Techniques of Automatic Control and Computer Engenering "STA'2014 Hammamet, Tunisia.

[13] A. Attou, A. Massoum and E. Chiali, "Sliding mode control of a permanent magnets synchronous machine", Fourth International Conference on Power Engineering, Energy and Electrical Drives (POWERENG), 2013.

[14] D. Bullo, A. Ferrara and M. Rubagotti, "Sliding mode observers for sensorless control of current-fed induction motors", 2011 American Control Conference on O'Farrell Street, San Francisco, CA, USA June/July 2011.

[15] H. Nademi, F. Tahami, M. Rezaei, "Fault tolerant IPMS motor drive based on adaptive backstepping observer with unknown stator resistance", 3rd IEEE Conference on Industrial Electronics and Applications, ICIEA 2008, 3-5 June 2008, pp: 1785 – 1790.

[16] R.Trabelsi, A.Khedher, M.F. Mimouni and F.M'Sahli, "An Adaptive Backstepping Observer for on-line rotor resistance adaptation", International Journal IJ-STA, Vol.4, N°1, July 2010, pp.1246-1267.

[17] P. Thayumanavan, R. Muthu and J. Sankararaman, "Sensorless field oriented control of wind turbine driven permanent magnet synchronous generator using flux linkage and back emf estimation methods," Research Journal of Applied Sciences, Engineering and Technology, Vol.7, N°.20, pp:4303-4312, 2014.

[18] W. Qiao, X. Yang and X. Gong, "Wind Speed and Rotor Position Sensorless Control for Direct-Drive PMG Wind Turbines," IEEE Transactions on Industry Applications, Vol.48, N°.1, January/February 2012.

[19] N. Khemiri, A. Khedher and M.F. Mimouni, "Wind energy conversion system using DFIG controlled by backstepping and sliding mode strategies", International Journal of Renewable Energy Research (IJRER), Vol.2, N°.3, pp: 421-430, 2012.

[20] M.A. Hamidaa, A. Glumineau and J. Leon, "Robust integral backstepping control for sensorless IPM synchronous motor controller", Journal of the Franklin Institute, Vol.349, N°.5, pp: 1734–1757, 2012.

[21] Karim A., Sam Ri, "A New Approach for Maximum Power Extraction from Wind Turbine Driven by Doubly Fed Induction Generator Based on Sliding Mode Control", Energy Management, Vol 1, N° 2, 2012.

[22] W. Qiao, X. Yang and X. Gong, "Wind Speed and Rotor Position Sensorless Control for Direct-Drive PMG Wind Turbines," IEEE Transactions on Industry Applications, Vol.48, N°.1, January/February 2012.

[23] J. Ben Alaya, A. Khedher and M.F. Mimouni, "DTC and Nonlinear Vector Control Strategies Applied to the DFIG operated at Variable Speed", WSEAS Transactions on environment and development. Vol. 6, N° 11, pp. 744-753, 2010.

[24] B. Belabbes, M.K. Fellah, A. Lousdad, A. Meroufel and A. Massoum, "Speed control by backstepping with nonlinear observer of a permanent magnet synchronous motor", Acta Electrotechnica et Informatica, Vol.6, N°.4, 2006.

[25] R. Galeazzi, M. P. S. Gryning and M. Blanke, "Observer backstepping control for variable speed wind turbine", American Control Conference (ACC), pp: 1036-1043, June 2013.

[26] A. Khedher, M.F. Mimouni, N. Derbel and A. Masmoudi, "A survey on modeling, estimation and on-line adaptation of induction motor parameters under R.F.O.C." Transactions on Systems, Signals and Devices, Vol.2, N° 2, pp.177–95, 2007.